Expression Profiling of Human Keratinocyte Response to Ultraviolet A: Implications in Apoptosis

Yu-Ying He, Jian-Li Huang, Robert H. Sik, Jie Liu[*], Michael P. Waalkes[*], and Colin F. Chignell
Laboratory of Pharmacology and Chemistry, National Institute of Environmental Health Sciences,[*] and Laboratory of Comparative Carcinogenesis, National Cancer Center at the National Institute of Environmental Health Sciences, NIH, Research Triangle Park, North Carolina, USA

Ultraviolet A radiation from sunlight is a major human health concern, as it is not absorbed by the ozone layer and can deeply penetrate into the skin causing skin damage. To study the molecular mechanism involved in the ultraviolet A effect, human HaCaT keratinocytes were exposed to ultraviolet A at doses of 10 J per cm^2 and 30 J per cm^2. Ultraviolet A irradiation caused dose- and time-dependent apoptotic cell death, as evidenced by DNA fragmentation, flow cytometry, and the activation of caspase-3. To study the genes altered by ultraviolet A at an apoptosis-inducing dose (30 J per cm^2), cells were harvested immediately after ultraviolet A treatment (0 h), and 6 h and 24 h after ultraviolet A exposure. Total RNA was extracted for microarray and real-time RT-PCR analysis, and cellular proteins were extracted for western blot analysis. Of the selected critical genes/proteins, the induction of c-Jun, c-myc, and p33[ING1], and the repression of epidermal growth factor receptor, inhibitor of apoptosis protein, and survivin pathways, could be involved in ultraviolet-A-induced apoptosis. On the other hand, the late induction of cyclin D1 and cyclin-dependent kinase 4 was indicative of possible cell cycle recovery in surviving cells. Real-time RT-PCR analysis confirmed these results and a majority of the protein levels paralleled their corresponding RNA levels. In addition, ultraviolet A treatment altered the expression of genes involved in signal transduction, RNA processing, structural proteins, and metabolism in a time-dependent manner. This initial microarray analysis could advance our understanding of cellular responses to ultraviolet A exposure, and provide a platform from which to further study ultraviolet-A-induced apoptosis and carcinogenesis.

Key words: apoptosis/carcinogenesis/keratinocytes/microarray/ultraviolet A.
J Invest Dermatol 122:533–543, 2004

Ultraviolet (UV) radiation from the sunlight that reaches the Earth's surface is a major environmental stress factor for human health, and the skin, as the physiologic barrier, is the main target of UV that may cause photoaging and skin carcinogenesis (Farr and Friedmann, 1986; Nataraj et al, 1995; Longstreth et al, 1998). The clinical and histologic characteristics of UV damage have long been known but the molecular mechanisms have only recently become the focus of concerted studies.

The UV portion of the solar electromagnetic spectrum is divided into UVC (200–280 nm), UVB (280–315 nm), and UVA (315–400 nm). UVC is absorbed completely by the stratospheric ozone layer and thus does not reach the Earth's surface. Although some UVB does reach the Earth's surface, most of it is absorbed by the ozone layer, and the UVB portion of UV in sunlight is small. The risk of UVB-induced acute and chronic damage, mainly mediated by DNA damage, can be minimized by avoiding direct exposure during midday hours, wearing protective hat/clothes, and using sunscreens (Pathak, 1996; Gasparro et al, 1998). UVA is not absorbed by the ozone layer, however, and constitutes more than 95% of solar UV radiation

reaching the Earth's surface. The lack of effective UVA sunscreens and the deeper penetration of UVA into skin increase the potential risk from exposure. A recent study has shown that UVA causes melanoma in fish (Setlow et al, 1993) and it could also be a risk factor in humans (Aubin et al, 2001; Wang et al, 2001).

The carcinogenic effects of UV irradiation may be decreased by apoptosis, or programmed cell death, which eliminates DNA-damaged or mutated cells. Recent studies using the microarray technique have revealed the global gene expression changes in keratinocytes caused by UVB (Catani et al, 2001; Li et al, 2001; Murakami et al, 2001; Valery et al, 2001; Sesto et al, 2002; Takao et al, 2002). Less is known about the impact of UVA on keratinocytes at the molecular level, however, especially the mechanisms associated with apoptosis. Here we have used the microarray technology to identify the genes that are affected by an apoptosis-inducing dose of UVA irradiation in human keratinocytes. Apoptosis in keratinocytes induced by simulated solar UVA irradiation at a dose equivalent to environmental exposure was investigated by gel electrophoresis of DNA fragmentation, caspase-3 activation, and flow cytometry. Real-time RT-PCR was used to validate the microarray results. Significantly, we have identified several categories of UVA-altered genes that are involved in apoptosis, signal transduction, RNA processing and translation, cell structure, and metabolism. We have also

examined the changes in protein levels corresponding to alterations in RNA levels. The results of this study provide important insights into the initial molecular response to UVA irradiation in potential target cells of UV carcinogenesis.

Results

UVA-induced apoptosis HaCaT cells were exposed to environmentally relevant doses (0–30 J per cm^2) of UVA radiation. In this regard, 30 J per cm^2 of UVA equates to about 1.5 h in the midday sun during summer at latitude 48°N (Jeanmougin and Civatte, 1987). Approximately 1 h 40 min was needed to obtain 30 J per cm^2 of UVA irradiation, depending upon the intensity of the source and the distance from the sample used in this study.

At 15 h after UVA exposure, cellular DNA was extracted and subjected to electrophoresis (Fig 1*A*). In UVA-irradiated HaCaT cells, a DNA ladder characteristic of apoptosis was detected at 30 J per cm^2, but not at lower doses. As expected, control cells showed intact DNA (Fig 1*A*). The number of apoptotic cells was also determined by DNA content as measured by flow cytometry (Fig 1*B*). UVA-induced apoptosis in HaCaT cells was both dose and time dependent. After 10 J per cm^2, the number of apoptotic cells increased slightly up to 24 h after UVA exposure, compared to the control cells. When cells were irradiated with 30 J per cm^2, however, the number of apoptotic cells increased rapidly, reaching 36% after 24 h of incubation.

One hour following UVA irradiation with 30 J per cm^2, cells clearly showed significant activation of caspase-3 (Fig 1*C*). After UVA irradiation with 10 J per cm^2, no activated caspase-3 was observed for up to 6 h, whereas at 24 h
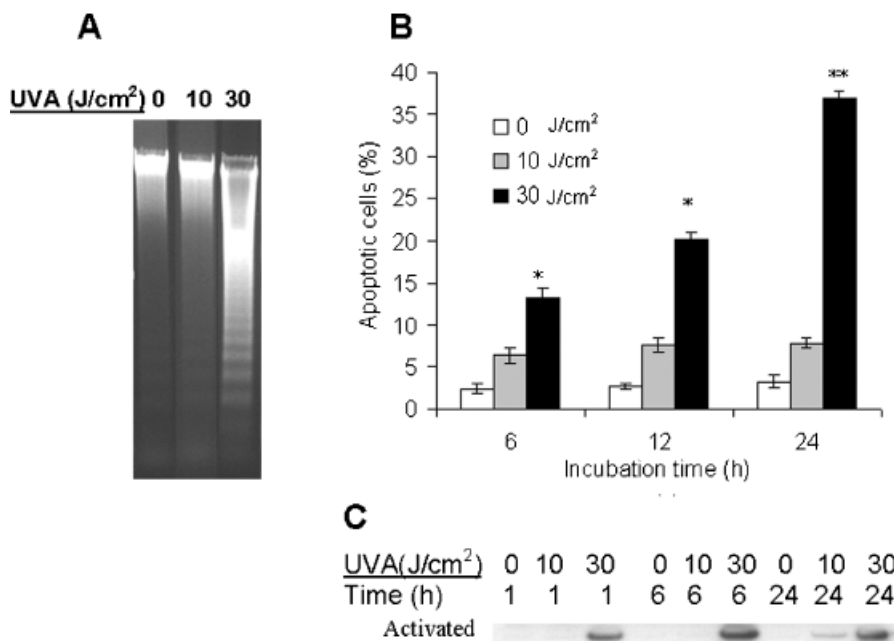
Figure 1
UVA-induced apoptosis in HaCaT cells. (*A*) HaCaT cells were irradiated with UVA (0, 10, and 30 J per cm^2). After incubation for 15 h, cells were harvested, and DNA fragmentation was analyzed on a 1.5% agarose gel. (*B*) After cells were treated with UVA at the indicated times, cells were stained with propidium iodide before being analyzed on a flow cytometer. The apoptotic percentage was obtained from the percentage of sub-G1 cell accumulation (*$p < 0.05$, **$p < 0.01$ compared to both control cells and cells irradiated with 10 J per cm^2 UVA). (*C*) After cells were treated with UVA and then incubated for the indicated times, cell lysates were analyzed on western blot with antibody to caspase-3.

Table I. Primer pairs used for real-time RT-PCR

Primer name	Forward primer (5′–3′)	Reverse primer (5′–3′)
Actin	ACTGGAACGGTGAAGGTGACA	ATGGCAAGGGACTTCCTGTAAC
CDK4	TCTGATGCGCCAGTTTCTAAGA	GCCATCTGGTAGCTGTAGATTCTG
c-Jun	CCCCCAGCGTATCTATATGGAA	GGTCACAGCACATGCCACTT
c-myc	GAGGCGAACACACAACGTCTT	CGCAACAAGTCCTCTTCAGAAA
EGFR	ACTATGTCCGGGAACACAAAGAC	GACATGCTGCGGTGTTTTCA
Fra1	GGAAGGAACTGACCGACTTCCT	CTTCCGGGATTTTGCAGATG
HIAP1	TGGACTCAGGTGTTGGGAATCT	GATGTGGATAGCAGCTGTTCAAGT
Keratin10	CGAGTCTTCATCTAAGGGACCAA	GAGACTCTCTCCTCTTGATGCAGTT
Keratin19	CAGGTCAGTGTGGAGGTGGATT	CCTCCCGGTTCAATTCTTCA
p33^{ING1}	GCCTGGTGTGAGGAGGACAA	CCCTATGAAAGGAATGGTTCCTT
PCNA	CATCCTCCAGCAGTCCGTTTA	TTGCCGGCGCATTTTAGTAT
Survivin	CAACTGTGCTCCTGTTTTGTCTTG	CCTTCTTCCTCCCTCACTTCTCA

Table II. Microarray analysis of gene expression alterations in HaCaT cells at 0, 6, and 24 h after the end of UVA irradiation

Gene bank number	Protein/gene	Time (h)		
		0	6	24
Apoptosis				
U45878	HIAP1	0.04	0.17	0.37
U75285	Survivin	0.38	0.60	0.87
V00568	c-myc	1.49	1.79	1.98
M15024	c-myb	4.32	2.21	4.72
M29039	jun-B	1.96	1.66	1.67
X16707	FRA1	7.64	9.65	8.21
J04111	c-Jun	6.01	4.13	3.04
J02958	met	0.41	0.23	1.50
X00663	EGFR	0.65	0.40	0.84
X57110	C-cbl	4.17	1.58	4.82
X95282	ρ-related GTP-binding protein ρE	1.89	1.65	0.87
X02751	N-ras	1.71	1.20	2.05
L20688	ρ GDI2	0.56	0.46	0.51
X57766	MMP11	1.56	1.45	2.68
Z46973	Phosphatidylinositol 3-kinase	0.09	0.20	0.24
X61498	NF-κB p100 subunit	1.18	1.28	2.16
M69043	MAD3	0.54	0.63	0.74
L78440	STAT4	0.95	3.58	4.15
U18671	STAT2	1.07	1.25	2.52
M22995	ras-related protein RAP-1 A	4.22	4.70	5.76
AF001954	p33ING1	1.32	1.65	2.46
DNA repair				
X74794	CDC21 homolog	0.45	0.61	0.79
M15796	PCNA	1.63	1.51	1.49
U35835	DNA-PK	0.39	0.36	0.51
M74524	Ubiquitin-conjugating enzyme E2 17 kDa (UBE2A)	0.60	0.75	0.95
M36067	DNA ligase I	0.46	0.34	0.63
D38551	KIAA0078	0.24	0.33	0.50
Cell cycle				
M25753	G2/mitotic-specific cyclin B1	0.64	0.36	0.67
L25676	Cell division protein kinase 9 (CDK9)	0.94	1.35	2.31
X66365	Cell division protein kinase 6 (CDK6)	1.26	0.83	1.41
M14505	Cyclin-dependent kinase 4 (CDK4)	1.11	0.88	1.38
M93311	Metallothionein-III (MT-III)	0.46	0.46	0.24
S72008	CDC10 protein homolog	0.48	0.33	0.60
U00001	CDC27HS protein	0.60	0.29	0.60
Signal transducer				
Y10479	E2F-3	2.82	2.11	2.36
U01351	Glucocorticoid receptor	0.06	0.28	0.36
L19872	Aryl hydrocarbon receptor (AH receptor)	0.43	0.42	0.54
Y07867	Pirin	0.25	0.18	0.19
X13403	oct-1	1.97	4.58	3.98

Table II. Continued

Gene bank number	Protein/gene	Time (h)		
		0	6	24
U65928	jun activation domain binding protein	0.65	0.63	0.87
U69127	Fuse-binding protein 3 (FBP3)	0.52	0.30	0.57
X52541	Early growth response protein 1 (hEGR1)	6.96	3.14	1.48
U03105	B4-2 protein	0.24	0.49	0.21
M59371	Ephrin type-A receptor 2 precursor	0.74	3.34	3.29
U84401	Smoothened; GX	1.61	0.81	3.22
U56998	Putative serine/threonine protein kinase PRK	14.42	3.00	4.84
M29870	p21-rac1	0.35	0.48	0.45
AF035752	Caveolin-2	0.45	0.29	0.50
Z18951	Caveolin-1	0.62	0.35	0.47
U59752	Cytohesin-1	0.38	0.24	0.81
U51004	Hint protein; protein kinase C inhibitor 1	0.37	0.52	0.48
RNA processing				
M31469	GTP-binding nuclear protein RAN (TC4)	0.78	0.58	0.78
U85625	Ribonuclease 6 precursor	0.55	0.74	0.55
X65372	Polypyrimidine tract-binding protein	1.27	0.76	0.72
U15782	Cleavage stimulation factor 77 kDa subunit	0.72	0.56	0.55
Translation				
U26032	Translation initiation factor eIF-2α subunit	0.71	0.36	0.44
M15353	EIF4E	0.56	0.65	0.47
D30658	Glycyl tRNA synthetase	0.77	0.47	0.74
J05032	Aspartyl-tRNA synthetase	0.23	0.31	0.32
Structural proteins				
X67081	Histone H4	0.99	0.33	0.47
M12623	HMG17	0.73	0.66	0.63
M34225	Type II cytoskeletal 8 keratin	0.64	0.60	0.56
X67683	Type II cytoskeletal 4 keratin	0.44	0.52	0.34
M99061	Type II cytoskeletal 2 epidermal keratin	0.79	0.70	0.53
M98776	Type II cytoskeletal 11 keratin	0.49	0.59	0.60
Y00503	Type I cytoskeletal 19 keratin	0.78	0.50	0.33
X52426	Type I cytoskeletal 13 keratin	0.48	0.51	0.22
M19156	Type I cytoskeletal 10 keratin	0.36	0.38	0.52
U59167	Desmin	0.51	0.29	0.26
Metabolism				
S80437	Fatty acid synthase	0.62	0.45	0.71
U27460	Uridine diphosphoglucose pyrophosphorylase	0.41	0.45	0.18
L16991	Thymidylate kinase	0.50	0.41	0.92
X59543	Ribonucleoside-diphosphate reductase M1 subunit	0.38	0.43	0.40
X00737	Purine nucleoside phosphorylase	1.42	2.04	1.78
U10860	GMP synthase; glutamine amidotransferase	0.39	0.28	0.43
U29656	DR-nm23	0.52	0.53	0.47
X66503	Adenylosuccinate synthetase	0.44	0.39	0.47

Results are expressed as the relative fold change of gene expression in cells at 0, 6, and 24 h after UVA (30 J per cm^2) exposure. The relative fold change was based on average values of four different hybridizations and significant from control (no UVA) using a 95% confidence level.

Figure 2
The clustering algorithm was used to group the time points and genes. The heights of the branches represent the relative similarities of the time points. The widths of the branches represent the relative similarities of the behavior patterns of individual genes responding to UVA irradiation. *Green* and *red* rectangles stand for repressed and induced values for individual genes, respectively. Genes that are altered significantly by UVA at 0, 6, and 24 h after exposure are presented. Some clusters are magnified for both repressed and induced genes. The scale is expressed as the log(2) of the relative fold compared to the control.
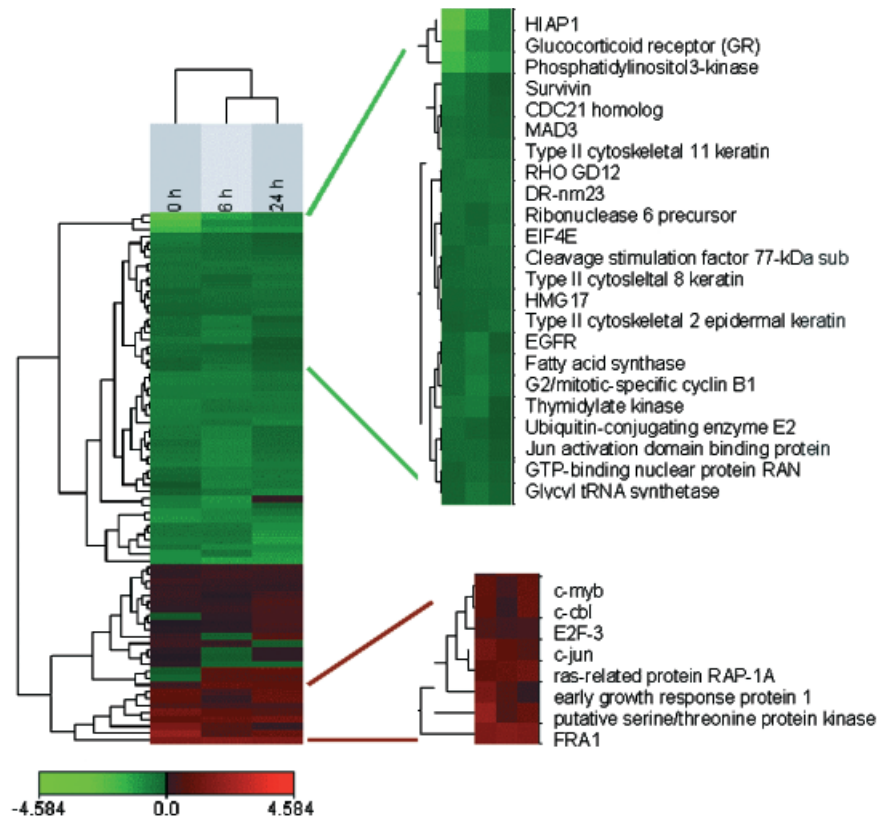
activated caspase-3 was detected by western blotting. The more rapid activation of caspase-3 induced by the higher dose of UVA (30 J per cm^2) is consistent with a significantly higher rate of apoptosis as shown by the DNA laddering and increased frequency of apoptotic cells by flow cytometry.

Microarray analysis of gene expression profiling in the response of HaCaT cells to UVA irradiation Cultured HaCaT cells were grown to subconfluence and exposed to 30 J per cm^2 UVA, which induced a significant apoptosis in HaCaT cells (see Fig 1). This dose of UVA was selected to focus on the molecular response to an apoptosis-inducing dose of UVA. After UVA exposure, the cells were harvested at 0, 6, and 24 h. Of the nearly 1200 genes present on the array, UVA induced aberrant expression in a wide variety of genes (see Table II). In fact, genes from various categories were differentially expressed at one or more time points after UVA exposure (Table II).

Using a clustering algorithm (Dysvik and Jonassen, 2001), the three time points after irradiation (Fig 2) were grouped. The most closely related were the 6 h and 24 h time points after UVA exposure. Some clusters of induced (*red*) and repressed (*green*) genes have been magnified and marked with gene names (Fig 2). More genes were repressed than induced. The different behaviors revealed by clustering analysis reflect the complexity of the UVA response and point towards the intricate processes that occur in response to UVA exposure. For conceptual purposes, the genes showing altered expression after UVA were classified according to their biologic function (see Table II). Some genes may have multiple functions, and some in the same category may have opposing roles (such as activators or inhibitors).

Correlations were sought between the expressed genes in functional groups and their expression patterns (activation/repression). There were several functional categories in which the genes behaved in a similar manner, indicating the existence of biologic processes globally altered by UVA exposure. A generalized suppression of expression was observed in the genes involved in RNA processing and translation, cell structure, and metabolism (Table II). In some categories, however, correlations are not evident, perhaps due to the complexity of responses (including genes involved in apoptosis, cell cycle, and DNA repair).

Confirmation of gene changes by real-time RT-PCR To evaluate the validity of the gene expression changes observed by microarray, critical genes and/or those showing highly altered expression after UVA were re-evaluated using real-time RT-PCR. Table III shows this comparison for 12 genes that were chosen based on either their function or their unusual response. In a majority of cases the direction of change after UVA is confirmed by real-time RT-PCR (Table III). UVA increased the expression of c-Jun, Fra1, c-myc, and p33^{ING1}, but decreased the expression of epidermal growth factor receptor (EGFR), human inhibitor of apoptosis protein 1 (HIAP1), and survivin, which may be involved in UVA-induced apoptosis. The transcript of cyclin D1 appeared to be unaltered whereas cyclin-dependent kinase 4 (CDK4) was induced at 24 h after UVA exposure. Proliferating cell nuclear antigen (PCNA) was induced after UVA. Keratins 10 and 19 were repressed by UVA radiation at 0, 6, and 24 h after exposure.

It should be noted that microarray analysis showed relative changes of less than 2-fold for at least one time point for a number of induced genes, including c-myc,

Table III. Comparisons between real-time RT-PCR and microarray analysis in examination of gene expression in cells irradiated with UVA

	Time (h)					
	0		**6**		**24**	
	PCR	**Array**	**PCR**	**Array**	**PCR**	**Array**
Apoptosis						
c-Jun	8.06	6.01***	2.63	4.13***	2.23	3.04**
Fra1	7.06	7.64***	13.18	9.65***	10.06	8.21***
c-Myc	1.24	1.49*	1.84	1.79***	2.02	1.98*
HIAP1	0.13	0.04**	0.03	0.17**	0.82	0.37*
Survivin	0.47	0.38*	0.53	0.60*	1.07	0.87
EGFR	0.30	0.65**	0.18	0.40***	0.66	0.84
p33^{ING1}	1.09	1.32	1.32	**1.65***	2.11	2.46*
Cell cycle						
Cyclin D1	1.27	1.58	0.85	0.84	0.94	1.11
CDK4	0.81	1.11	0.82	0.88	1.75	1.38*
DNA repair						
PCNA	1.75	1.63*	1.24	1.51***	0.84	1.49**
Keratins						
Keratin 10	0.50	0.36***	0.49	0.38***	0.67	0.52***
Keratin 19	0.48	0.78*	0.35	0.50***	0.31	0.33***

Data are expressed as fold increase change to control (no UVA), which is set to 1.0. PCR, real-time RT-PCR; Array, microarray analysis. Real-time PCR and microarray were compared to determine the relative fold change of gene expression in cells treated with UVA (30 J per cm^2), compared to the respective control. Genes were identified as induced or repressed compared to the respective controls at at least one time point after UVA exposure using a 95% confidence level. Reverse transcription was performed using SYBR Green detection for all genes. Microarray analysis relative fold change was based on average values of four different hybridizations, and significance from control is signified as
*$p < 0.05$,
**$p < 0.01$,
***$p < 0.001$. Standard errors are omitted for clarity.

PCNA, p33^{ING1}, and CDK4, which were confirmed by real-time RT-PCR to be less than 2-fold. Among the 36 comparisons between microarray and RT-PCR after UVA, the only one that was inconsistent was PCNA at 24 h, which was significantly induced in microarray analysis but found to be unchanged by real-time RT-PCR.

For genes repressed by UVA exposure, real-time RT-PCR results were in good agreement with those from microarrays. There were several examples of genes that the microarray analysis showed as not significantly altered at one or more time points (EGFR, 24 h; CDK4, 0 h; and CDK4, 6 h), but that were either induced or repressed as detected using real-time RT-PCR analysis. The relative fold changes for c-Jun (0 h) and Fra1 (6 h and 24 h) were higher in real-time RT-PCR than microarray analysis. This effect may be caused by saturation at the high-density range of the radiographic detection of microarray hybridization.

Effects of UVA on selected translational products Although microarray hybridizations measure changes in RNA levels, it is the eventual changes in protein levels that directly impact cellular functions. We used western blots to assess the changes in protein levels for selected critical genes (Fig 3). The cells were irradiated with 10 or 30 J per cm^2 UVA and then incubated for 1, 6, or 24 h. Protein levels

of c-JUN and c-MYC exhibited significant increases that were maximal at 6 h. In contrast, EGFR decreased at both 6 h and 24 h after UVA. The protein level of the newly identified tumor suppressor protein p33^{ING1} increased at 6 and 24 h after UVA, which paralleled RNA levels of this gene. The antiapoptotic proteins IAP and survivin decreased at 24 h after UVA exposure. IAP and survivin did not show any change in protein levels up to 6 h after irradiation, however, although corresponding RNA levels decreased.

After UVA irradiation the protein level of cyclin D1 decreased to a very low level at 1 h but increased at 24 h. This pattern could be due to its predominant post-translational regulation (Luo *et al*, 2003). The protein levels of CDK4 increased at 24 h, which is consistent with its RNA levels.

Discussion

In this work, the human keratinocyte cell line HaCaT was used to investigate the initial molecular response to UVA irradiation. Although HaCaT cells are spontaneously immortalized through p53 mutation, evidence suggests that this cell line closely approximates normal keratinocytes in terms of differentiation (Boukamp *et al*, 1988). HaCaT cells have also provided a valuable model system for the study of
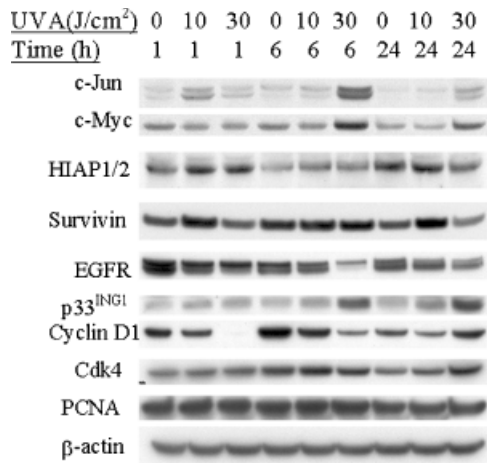
Figure 3
The changes in protein levels of selected genes. The cells were starved 15 h in 1% FBS/DMEM and then irradiated with UVA (10 and 30 J per cm^2). At indicated times after irradiation cells were harvested and equal protein was subjected to western blotting. β-Actin was used as an internal loading control in a parallel gel.

the molecular events associated with malignant transformation of human epithelial cells (Boukamp et al, 1988). Indeed HaCaT cells have been used extensively as an *in vitro* model of epidermal skin to investigate the effects of UVB and UVA (Catani et al, 2001; Phillipson et al, 2002). Thus, in this study, we have employed HaCaT cells to help define altered gene expression induced by UVA exposure in order to provide insight into the initial molecular response in a potential target cell model of UV carcinogenesis.

We have shown that UVA exposure (25 J per cm^2) induced apoptosis in HaCaT keratinocytes and this process is regulated by intracellular redox status due to GSH efflux (He et al, 2003). In this study we have used a higher dose of UVA (30 J per cm^2) to investigate gene expression altered by UVA in human HaCaT keratinocytes. Whereas only a slight increase in apoptotic cells was observed at 10 J per cm^2 UVA, at 30 J per cm^2 36% of cells underwent apoptosis by 24 h after UVA irradiation (Fig 1*B*). As early as 1 h after exposure, activation of caspase-3, one key enzyme dedicated to apoptosis, was observed. This indicates that apoptosis was initiated by UVA exposure at an early time. Gene expression pattern showed that UVA induced early responses of gene expression immediately after exposure and late response between 6 h and 24 h after exposure.

Genes involved in apoptosis Two antiapoptotic genes were significantly altered by UVA exposure, which previously were not known to respond to UV radiation in keratinocytes. From 0 to 24 h after irradiation, two antiapoptotic genes related to the baculovirus *iap* gene (Duckett et al, 1996; Uren et al, 1996) were repressed: HIAP1, and apoptosis inhibitor survivin. HIAP1 is known to bind and inhibit the activated forms, but not the proenzyme forms, of caspase-3 and caspase-7 (Deveraux et al, 1997, 1998; Roy et al, 1997). Survivin is thought to inhibit apoptosis through different pathways from Bcl-2 and its expression may influence both epidermal homeostasis and the development of skin cancer (Chiodino et al, 1999). Thus suppression of the expression of either of these genes could

enhance apoptotic rate. The inconsistency between their RNA levels and corresponding protein levels may result from the time required for gene expression to result in protein translation/production.

UVA caused strong and persistent induction of the expression of c-myc, c-Jun, and Fra1, jun-B, C-cbl, and myb oncogenes. Western blotting results show that the protein levels of c-MYC and c-JUN are induced at 6 h and 24 h after the end of UVA exposure. The protein products of many dominant oncogenes are capable of inducing both cell proliferation and apoptosis. For example, c-myc is able to induce malignant transformation and apoptosis; deregulated expression of c-myc not only promotes proliferation but also can either induce or sensitize cells to apoptosis (Evan et al, 1992; Amundson et al, 1998; Hoffman and Liebermann, 1998; Felsher and Bishop, 1999; Pelengaris et al, 2000). More recent research on c-myc has focused on how it drives apoptosis. It has been proposed that c-myc induces apoptosis through separate "death priming" and "death triggering" mechanisms in which "death priming" and mitogenic signals are coordinated (Prendergast, 1999). In addition, c-Jun expression and c-Jun/AP-1 activation were found to be associated with ionizing-radiation-induced apoptosis in the developing cerebellum of the rat (Ferrer et al, 1995; 1996). Wang and coworkers found that specific expression of c-Jun is a sufficient trigger for endothelial cells to undergo apoptosis (Wang et al, 1999). Thus many of these oncogenes have dual roles in proliferation and apoptosis and these data serve to point out the complexity of the molecular response to UV irradiation.

The expression and its corresponding protein level of the newly identified tumor suppressor gene p33^{ING1} (Garkavtsev et al, 1996) is persistently induced by UVA irradiation. p33^{ING1} levels have been previously found to increase upon the induction of apoptosis in P19 teratocarcinoma cells by serum deprivation and the pathway by which ING1 modulates cell death is synergistic with myc-dependent apoptosis (Helbing et al, 1997). Increased p33^{ING1} levels may increase the cell's sensitivity to apoptosis and therefore reduce UVA-induced malignant transformation in keratinocytes (Shinoura et al, 1999). A recent study has shown that p33^{ING1} shares many biologic functions with p53, including mediation of growth arrest and apoptosis as well as DNA repair (Cheung et al, 2001). The expression of p33^{ING1} appears independent of p53 status, considering the lack of wild-type p53 function in HaCaT cells (Cheung et al, 2000). The overexpression of p33^{ING1} promotes p53-independent and c-myc-inducible apoptosis (Helbing et al, 1997), which is consistent with our results, i.e., that the induction of p33^{ING1} and c-myc protein levels could be synergistic with UVA-induced apoptosis.

On the other hand, EGFR, a gene involved in cell survival and proliferation, is persistently repressed by UVA irradiation. In parallel, its corresponding protein levels decreased at 6 and 24 h after UVA exposure. Decreased EGFR signaling may enhance the apoptotic response by increasing the cell's sensitivity to apoptotic stimuli (Modjtahedi et al, 1998; Qiao et al, 2001). Apoptosis could be triggered by downregulation of EGFR (Brabyn and Kleine, 1995). Phosphatidylinositol 3-kinase, a gene involved in cell survival, was suppressed by UVA. The suppressed expres-

sion of phosphatidylinositol 3-kinase could reduce the survival pathway and thereby enhance apoptosis after UVA exposure (Edwards *et al*, 2002; Liu *et al*, 2002).

Cell cycle and DNA repair As expected, the effect of UVA irradiation on the expression of genes involved in the cell cycle was complex. UVA caused the decreased expression of cyclin B1, CDC27HS, CDC10 protein homolog, and MT-III. The expression of other genes, however, such as CDK4, CDK6, CDK9, was induced at 24 h after exposure. RNA levels of cyclin D1 are not altered up to 24 h after UVA whereas its corresponding protein levels show decreases at the early time and increases at 24 h after exposure. These findings suggest that, after a short delay, cell cycle arrest may occur after UVA exposure. Presumably such a delay would be due to insufficient DNA repair for the cell cycle to proceed. As a result, the cells undergo either cell cycle arrest or apoptosis. The latter was demonstrated by the DNA laddering, flow cytometry, and activation of caspase-3 (see Fig 1).

Cyclin D1 and CDK4 are proteins involved in the G1/S cell cycle progression. These two proteins are typically classified as late response genes, compared to c-Jun, Fra1, or c-myc. PCNA was very abundant in control cells. The inconsistency between gene transcript levels and translation products of some genes reflect the complexity of the molecular response to UVA irradiation. There is clearly a complex interplay of gene expression and epigenetic control factors that occurs with UVA irradiation, even at environmentally relevant levels. Post-translational regulation processes caused by UVA exposure may also contribute to the inconsistency between protein and RNA levels.

Of the genes involved in DNA repair and synthesis on the microarray, several were differentially expressed after UVA irradiation. UVA induced the expression of PCNA, which is involved in DNA replication and is present at very high levels in control keratinocytes. Another gene involved in DNA replication, namely the CDC21 homolog, was repressed immediately after irradiation and at 6 h thereafter. UVA suppressed expression of UBE2A, DNA-PK, and DNA ligase I. Although the cells sensed the damaging stimuli and responded by inducing the repairing machinery, the UVA dose used activated the apoptosis machinery as early as 1 h after UVA exposure. The initiation and execution of apoptosis could shut down some of the repair genes as a secondary response. These proteins play a role in the cell cycle arrest that allows cells to repair their DNA damage and presumably coordinate DNA repair with the cell cycle.

Signal transduction, RNA processing and translation, cell structure, and metabolism In keratinocytes, genes producing various signal transducers and transcription factors also show complex expression patterns after UVA. The transcription factors induced by UVA were E2F, oct-1, and hEGR1. In contrast, pirin (the most predominant NFI/CTF1 interactor (Wendler *et al*, 1997)), the expression of AH receptor, FBP3, glucocorticoid receptor, and the jun activation domain binding protein were all suppressed. This again serves to point out the variety of molecular processes that are influenced by UVA irradiation.

In contrast, UVA irradiation suppressed the expression of genes involved in RNA processing and translation, cell structure, and metabolism. The generalized decrease of transcripts involved in translation provided additional evidence that the experimental conditions we employed did induce a significant level of apoptosis, as this process rapidly inhibits the rate of protein synthesis at the level of polypeptide chain initiation (Clemens *et al*, 2000).

Genes encoding for cytoskeletal proteins showed a generalized tendency towards suppression by UVA, including type I and type II cytoskeletal keratins. Keratin 10 is characteristic of differentiated cells and was suppressed by UVA, suggesting that UVA also inhibited the differentiation of keratinocytes, which could be involved in skin tumorigenesis in the population of surviving cells (Santos *et al*, 2002). Keratin 19 is synthesized mainly in embryonic and adult simple epithelia, but has also been found in stratified epithelia. Keratin 19 expression does not irrevocably commit a cell to any one of the local differentiation options. Such predicted differentiational flexibility is proposed to imply vulnerability to transformation (Stasiak *et al*, 1989). It has been reported previously that the expression of keratin 19 is abnormal in many of the squamous cell carcinoma cell lines, and the correlation between RAR β gene expression and keratin 19 gene expression that has been observed in the various normal keratinocyte subtypes from the oral cavity has been shown to be absent in transformed keratinocytes (squamous cell carcinoma cells) (Hu *et al*, 1991). The significance of reduced keratin expression after UVA remains to be determined, however. The generalized suppression of keratin genes could also be the consequence of the initiation of apoptotic machinery, in order to coordinate the cytoskeletal protein production with the apoptosis-associated morphologic changes in the presence of keratin fragmentation by caspase activation in apoptosis (Ku *et al*, 1997).

The expression of the genes encoding metabolic enzymes was suppressed by UVA. This was true for those related to nucleotide, lipid, or amino acid metabolism. The reduced expression of DR-nm23, which is involved in the phosphorylation of nucleoside diphosphates, could play a role in UVA-induced apoptosis in keratinocytes (Venturelli *et al*, 1995). The roles of these metabolism-related genes in UVA-induced apoptosis as well as carcinogenesis remain to be defined.

In summary, apoptosis-inducing UVA induced the early molecular response of keratinocytes to UVA exposure. Thus many, but not all, the gene activations or inactivations observed with UVA in this study may contribute to an apoptotic response. The apoptosis-inducing UVA dose induced early response proteins such as c-Jun, c-myc, and p33^{ING1}, but repressed EGFR. HIAP1 was also repressed at the later time. These changes in gene expression could be involved in the UVA-induced apoptosis process. The late induction of cyclin D1 and CDK4 protein levels suggests that surviving cells may begin to re-enter the cell cycle, which could facilitate the preservation of mutations resulting from UVA and result (Robert *et al*, 1996; Emri *et al*, 2000; Aubin *et al*, 2001; Phillipson *et al*, 2002), eventually, in tumor development. In addition, generalized repression was observed in many genes encoding for

structural proteins, and genes involved in RNA processing and translation, as well as those concerned with cellular metabolism. These results reveal the molecular response to UVA exposure in keratinocytes and serve as a basis for undertaking investigations into the characterization of UVA-altered genes and molecular pathways that may be involved in UVA-associated carcinogenesis.

Materials and Methods

Cell culture HaCaT cells (Boukamp *et al*, 1988) were obtained from Professor N. Fusenig (German Cancer Research Center, Heidelberg, Germany) and maintained in monolayer culture in 95% air/5% CO_2 at 37°C in Dulbecco's modified Eagle's medium (DMEM) supplemented with 10% fetal bovine serum (FBS), 31 μg per mL penicillin, and 50 μg per mL streptomycin. Cells were grown in plastic Petri dishes (100 mm) for 24–48 h and used at 50%–70% confluence.

UVA treatment The medium was removed and cells were washed once with sterile phosphate-buffered saline. After the addition of phosphate-buffered saline containing 10 mM glucose, the cells were irradiated (Gasparro and Brown, 2000) with fluorescent lamps (Houvalite F20T12BL-HO PUVA, National Biological, Twinsburg, OH) with the dish lid on. The UVA dose was monitored through the lid of the Petri dish used for the experiments with a Goldilux UV meter equipped with a UVA detector (Oriel Instruments, Stratford, CT). Control samples were kept in the dark under the same conditions. After treatment, fresh medium was added after exposure and the cells were incubated at 37°C. The cells were harvested immediately after the end of UVA exposure (0 h), and then 1 h, 6 h, or 24 h after the end of UVA exposure.

DNA fragmentation The pattern of DNA cleavage was analyzed by agarose gel electrophoresis. Briefly, cell pellets were resuspended in lysis buffer (5 mM Tris−HCl pH 8.0; 20 mM ethylenediamine tetraacetic acid; 0.5% Triton X-100) and incubated on ice at 4°C overnight. After incubation at 56°C for 1 h with RNase A (100 μg per mL) and then for 1 h with proteinase K (200 μg per mL), the cell lysate was extracted with phenol/chloroform/isopropyl alcohol (25:24:1, vol/vol). DNA was precipitated with ethanol and subsequently washed with 70% ethanol. DNA samples, dissolved in 1 × TE buffer, were separated by horizontal electrophoresis on 1.5% agarose gels, stained with ethidium bromide, and visualized under UV light.

Flow cytometry Apoptosis was measured by determining the DNA content of the cells by propidium iodide staining and flow cytometry, as previously described (Denning *et al*, 1998). Briefly, cells were trypsinized, fixed with ethanol, and stained with propidium iodide before being analyzed by flow cytometry using a Becton Dickinson FACSort (Becton Dickinson, Mountain View, CA). Cells with a DNA content less than the G1 amount (i.e., sub G_0) of untreated cells were considered apoptotic.

RNA extraction Total RNA was isolated by using TRIzol (Gibco/BRL Life Technologies). The total RNA was then subjected to DNase digestion by using RNase-Free DNase Set (Qiagen, Valencia, CA) followed by cleanup with the RNeasy Mini kit (Qiagen). The resultant DNA-free RNA was quantitated by UV spectroscopy at 260 nm and stored in RNase-free H_2O at −70°C. Samples were separated by electrophoresis on formaldehyde denaturing agarose gels stained with ethidium bromide to confirm the integrity of the 28S and 18S ribosomal RNA. The DNA-free total RNA was used for microarray and real-time RT-PCR analysis.

Microarray hybridization Atlas Human Cancer 1.2 microarray analyses were performed according to the manufacturer's instructions (Clontech, Palo Alto, CA). All hybridizations were carried out in quadruplicate. Before labeling, RNA samples from two biologic replicates were pooled in equal amounts.

Briefly, total DNA-free RNA was converted to [α-^{32}P]-dATP-labeled cDNA probe using MMLV reverse transcriptase and the Atlas Human Cancer CDS primer mix. The ^{32}P-labeled cDNA probe was purified using NucleoSpin columns (Clontech). The membrane was prehybridized with Expresshyb (Clontech) for 60 min at 68°C, followed by hybridization with probe overnight at 68°C. The arrays were washed four times in 2 × sodium citrate/chloride buffer (SSC)/0.1% sodium dodecyl sulfate (SDS), 30 min each, and two times in 0.1 × SSC/0.1% SDS. The arrays were then sealed in plastic wrap and exposed to a Molecular Dynamics Phosphoimage screen (Amersham Pharmacia, Piscataway, NJ) or to radiographic film. The images were analyzed densitometrically using AtlasImage software (Clontech). The gene expression intensities were normalized with the sum of nine housekeeping genes on the array. Comparisons between control and UVA-irradiated samples were made by Student *t* test. $p < 0.05$ was considered statistically significant. The description of the methodology used in this study conforms to the MIAME (Minimal Information to Annotate a Microarray Experiment).

Real-time RT-PCR Quantitative real-time PCR was conducted as described previously (Walker, 2001; Martinez *et al*, 2002). Briefly, total RNA was reverse transcribed using reverse transcription reagents (PE Applied Biosystems, Foster City, CA). The resulting cDNA was used in subsequent real-time PCR reactions. Real-time fluorescence detection was carried out using an ABI Prism 7700 Sequence Detection System. Reactions were carried out in microAmp 96-well reaction plates using SYBR Green DNA PCR Core Reagent kit (PE Applied Biosystems). All primers were designed using PrimerExpress Software (PE Applied Biosystems) (see Table I). Samples were analyzed in triplicate, avnd β-actin was used as an endogenous control. Fold induction was calculated using the formula $2^{-\Delta\Delta C_T}$, where ΔC_T = target gene C_T − β-actin C_T, and $\Delta\Delta^{CT}$ is based on the mean ΔC_T of the control (non-UVA treated). The C_T value is determined as the cycle at which the fluorescence signal emitted is significantly above background levels and is inversely proportional to the initial template copy number.

Western blotting Cells (3×10^6) were seeded in plastic Petri dishes, grown for 24 h, and then starved for 15 h in 1% serum-DMEM. After UVA irradiation, 1% serum-DMEM was given and cells were incubated for indicated periods. Cells from control or UVA treatment were harvested and lyzed with M-PER Mammalian Protein Extraction Reagent (Pierce, Rockford, CA) supplemented with Protease Inhibitor Cocktail (Calbiochem, San Diego, CA). Total cell lysates were clarified by centrifugation at 15,000 × *g* for 10 min at 4°C. Protein concentrations were determined using BCA assay (Pierce).

Equal amounts of protein (40–80 μg) were subjected to electrophoresis on NuPage precast gels (4%–12%) (Novex, San Diego, CA), followed by electrophoretic transfer to nitrocellulose membranes. Membranes were blocked in 5% nonfat milk in TBST (15 mM Tris−HCl, pH 7.4, 150 mM NaCl, and 0.1% Tween 20) for 2 h at room temperature, followed by incubation with primary antibody for 1 h at room temperature. Membranes were then washed with TBST, and incubated with secondary antibody (Santa Cruz Biotechnology, Santa Cruz, CA) for 1 h at room temperature. After washing again with TBST, proteins were visualized using SuperSignal chemiluminescent substrate (Pierce).

Antibodies used were as follows: caspase-3 (E-8), c-Jun (D), c-myc (N-262), EGFR 1005, p33^{ING1} (c-19), CDK4 (H-22), IAP1/2 (A-13), and survivin (D-8) from Santa Cruz Biotechnology; β-actin from Sigma (St Louis, MO).

Address correspondence to: Yu-Ying He, Laboratory of Pharmacology and Chemistry, National Institute of Environmental Health Sciences, NIH, Research Triangle Park, North Carolina. Email: he3@niehs.nih.gov

References

Amundson SA, Zhan Q, Penn LZ, Fornace AJ Jr: Myc suppresses induction of the growth arrest genes gadd34, gadd45, and gadd153 by DNA-damaging agents. Oncogene 17:2149–2154, 1998

Aubin F, Humbey O, Humbert P, Laurent R, Mougin C: Melanoma. Role of ultraviolet radiation: From physiology to pathology. Presse Med 30:546–551, 2001

Boukamp P, Petrussevska RT, Breitkreutz D, Hornung J, Markham A, Fusenig NE: Normal keratinization in a spontaneously immortalized aneuploid human keratinocyte cell line. J Cell Biol 106:761–771, 1988

Brabyn CJ, Kleine LP: EGF causes hyperproliferation and apoptosis in T51B cells: Involvement of high and low affinity EGFR binding sites. Cell Signal 7:139–150, 1995

Catani MV, Rossi A, Costanzo A, Sabatini S, Levrero M, Melino G, Avigliano L: Induction of gene expression via activator protein-1 in the ascorbate protection against UV-induced damage. Biochem J 356:77–85, 2001

Cheung KJ Jr, Bush JA, Jia W, Li G: Expression of the novel tumour suppressor p33 (ING1) is independent of p53. Br J Cancer 83:1468–1472, 2000

Cheung KJJ, Mitchell D, Lin P, Li G: The tumor suppressor candidate p33 (ING1) mediates repair of UV-damaged DNA. Cancer Res 61:4974–4977, 2001

Chiodino C, Cesinaro AM, Ottani D, Fantini F, Giannetti A, Trentini GP, Pincelli C: Communication: Expression of the novel inhibitor of apoptosis survivin in normal and neoplastic skin. J Invest Dermatol 113:415–418, 1999

Clemens MJ, Bushell M, Jeffrey IW, Pain VM, Morley SJ: Translation initiation factor modifications and the regulation of protein synthesis in apoptotic cells. Cell Death Differ 7:603–615, 2000

Denning MF, Wang Y, Nickoloff BJ, Wrone-Smith T: Protein kinase Cδ is activated by caspase-dependent proteolysis during ultraviolet radiation-induced apoptosis of human keratinocytes. J Biol Chem 273:29995–30002, 1998

Deveraux QL, Takahashi R, Salvesen GS, Reed JC: X-linked IAP is a direct inhibitor of cell-death proteases. Nature 388:300–304, 1997

Deveraux QL, Roy N, Stennicke HR, *et al*: IAPs block apoptotic events induced by caspase-8 and cytochrome c by direct inhibition of distinct caspases. Embo J 17:2215–2223, 1998

Duckett CS, Nava VE, Gedrich RW, *et al*: A conserved family of cellular genes related to the baculovirus iap gene and encoding apoptosis inhibitors. Embo J 15:2685–2694, 1996

Dysvik B, Jonassen I: J-Express: Exploring gene expression data using Java. Bioinformatics 17:369–370, 2001

Edwards E, Geng L, Tan J, Onishko H, Donnelly E, Hallahan DE: Phosphatidy-linositol 3-kinase/Akt signaling in the response of vascular endothelium to ionizing radiation. Cancer Res 62:4671–4677, 2002

Emri G, Wenczl E, Van Erp P, Jans J, Roza L, Horkay I, Schothorst AA: Low doses of UVB or UVA induce chromosomal aberrations in cultured human skin cells. J Invest Dermatol 115:435–440, 2000

Evan GI, Wyllie AH, Gilbert CS, *et al*: Induction of apoptosis in fibroblasts by c-myc protein. Cell 69:119–128, 1992

Farr PM, Friedmann PS: Solar radiation-induced disorders. In: Thody AJ, Friedmann PS, (eds). Scientific Basis of Dermatology. London: Churchill Livingstone, 1986; p 262–289

Felsher DW, Bishop JM: Transient excess of MYC activity can elicit genomic instability and tumorigenesis. Proc Natl Acad Sci USA 96:3940–3944, 1999

Ferrer I, Barron S, Rodriquez-Farre E, Planas AM: Ionizing radiation-induced apoptosis is associated with c-Jun expression and c-Jun/AP-1 activation in the developing cerebellum of the rat. Neurosci Lett 202:105–108, 1995

Ferrer I, Olive M, Blanco R, Cinos C, Planas AM: Selective c-Jun overexpression is associated with ionizing radiation-induced apoptosis in the developing cerebellum of the rat. Brain Res Mol Brain Res 38:91–100, 1996

Garkavtsev I, Kazarov A, Gudkov A, Riabowol K: Suppression of the novel growth inhibitor p33ING1 promotes neoplastic transformation. Nat Genet 14:415–420, 1996

Gasparro FP, Brown DB: Photobiology 102. UV sources and dosimetry – The proper use and measurement of "photons as a reagent". J Invest Dermatol 114:613–615, 2000

Gasparro FP, Mitchnick M, Nash JF: A review of sunscreen safety and efficacy. Photochem Photobiol 68:243–256, 1998

He Y, Huang JL, Ramirez DC, Chignell CF: Role of reduced glutathione efflux in apoptosis of immortalized human keratinocytes induced by UVA. J Biol Chem 278:8058–8064, 2003

Helbing CC, Veillette C, Riabowol K, Johnston RN, Garkavtsev I: A novel candidate tumor suppressor, ING1, is involved in the regulation of apoptosis. Cancer Res 57:1255–1258, 1997

Hoffman B, Liebermann DA: The proto-oncogene c-myc and apoptosis. Oncogene 17:3351–3357, 1998

Hu L, Crowe DL, Rheinwald JG, Chambon P, Gudas LJ: Abnormal expression of retinoic acid receptors and keratin 19 by human oral and epidermal squamous cell carcinoma cell lines. Cancer Res 51:3972–3981, 1991

Jeanmougin M, Civatte J: Dosimetry of solar ultraviolet radiation. Daily and monthly changes in Paris. Ann Dermatol Venereol 114:671–676, 1987

Ku NO, Liao J, Omary MB: Apoptosis generates stable fragments of human type I keratins. J Biol Chem 272:33197–33203, 1997

Li D, Turi TG, Schuck A, Freedberg IM, Khitrov G, Blumenberg M: Rays and arrays: The transcriptional program in the response of human epidermal keratinocytes to UVB illumination. FASEB J 15:2533–2535, 2001

Liu W, Chin-Chance C, Lee EJ, Lowe WL Jr: Activation of phosphatidylinositol 3-kinase contributes to insulin-like growth factor I-mediated inhibition of pancreatic β-cell death. Endocrinology 143:3802–3812, 2002

Longstreth J, de Gruijl FR, Kripke ML, *et al*: Health risks. J Photochem Photobiol B 46:20–39, 1998

Luo H, Zhang J, Dastvan F, *et al*: Ubiquitin-dependent proteolysis of cyclin D1 is associated with coxsackievirus-induced cell growth arrest. J Virol 77:1–9, 2003

Martinez JM, Afshari CA, Bushel PR, Masuda A, Takahashi T, Walker NJ: Differential toxicogenomic responses to 2,3,7,8-tetrachlorodibenzo-p-dioxin in malignant and nonmalignant human airway epithelial cells. Toxicol Sci 69:409–423, 2002

Modjtahedi H, Affleck K, Stubberfield C, Dean C: EGFR blockade by tyrosine kinase inhibitor or monoclonal antibody inhibits growth, directs terminal differentiation and induces apoptosis in the human squamous cell carcinoma HN5. Int J Oncol 13:335–342, 1998

Murakami T, Fujimoto M, Ohtsuki M, Nakagawa H: Expression profiling of cancer-related genes in human keratinocytes following non-lethal ultraviolet B irradiation. J Dermatol Sci 27:121–129, 2001

Nataraj AJ, Trent JC 2nd, Ananthaswamy HN: p53 gene mutations and photocarcinogenesis. Photochem Photobiol 62:218–230, 1995

Pathak MA: Sunscreens: Progress and perspectives on photoprotection of human skin against UVB and UVA radiation. J Dermatol 23:783–800, 1996

Pelengaris S, Rudolph B, Littlewood T: Action of Myc *in vivo* – Proliferation and apoptosis. Curr Opin Genet Dev 10:100–105, 2000

Phillipson RP, Tobi SE, Morris JA, McMillan TJ: UV-A induces persistent genomic instability in human keratinocytes through an oxidative stress mechanism. Free Radic Biol Med 32:474–480, 2002

Prendergast GC: Mechanisms of apoptosis by c-Myc. Oncogene 18:2967–2987, 1999

Qiao L, Studer E, Leach K, *et al*: Deoxycholic acid (DCA) causes ligand-independent activation of epidermal growth factor receptor (EGFR) and FAS receptor in primary hepatocytes: Inhibition of EGFR/mitogen-activated protein kinase-signaling module enhances DCA-induced apoptosis. Mol Biol Cell 12:2629–2645, 2001

Robert C, Muel B, Benoit A, Dubertret L, Sarasin A, Stary A: Cell survival and shuttle vector mutagenesis induced by ultraviolet A and ultraviolet B radiation in a human cell line. J Invest Dermatol 106:721–728, 1996

Roy N, Deveraux QL, Takahashi R, Salvesen GS, Reed JC: The c-IAP-1 and c-IAP-2 proteins are direct inhibitors of specific caspases. Embo J 16:6914–6925, 1997

Santos M, Paramio JM, Bravo A, Ramirez A, Jorcano JL: The expression of keratin k10 in the basal layer of the epidermis inhibits cell proliferation and prevents skin tumorigenesis. J Biol Chem 277:19122–19130, 2002

Sesto A, Navarro M, Burslem F, Jorcano JL: Analysis of the ultraviolet B response in primary human keratinocytes using oligonucleotide microarrays. Proc Natl Acad Sci USA 99:2965–2970, 2002

Setlow RB, Grist E, Thompson K, Woodhead AD: Wavelengths effective in induction of malignant melanoma. Proc Natl Acad Sci USA 90:6666–6670, 1993

Shinoura N, Muramatsu Y, Nishimura M, *et al*: Adenovirus-mediated transfer of p33ING1 with p53 drastically augments apoptosis in gliomas. Cancer Res 59:5521–5528, 1999

Stasiak PC, Purkis PE, Leigh IM, Lane EB: Keratin 19: Predicted amino acid sequence and broad tissue distribution suggest it evolved from keratinocyte keratins. J Invest Dermatol 92:707–716, 1989

Takao J, Ariizumi K, Dougherty II, Cruz PD Jr: Genomic scale analysis of the human keratinocyte response to broad-band ultraviolet-B irradiation. Photodermatol Photoimmunol Photomed 18:5–13, 2002

Uren AG, Pakusch M, Hawkins CJ, Puls KL, Vaux DL: Cloning and expression of apoptosis inhibitory protein homologs that function to inhibit apoptosis and/or bind tumor necrosis factor receptor-associated factors. Proc Natl Acad Sci USA 93:4974–4978, 1996

Valery C, Grob JJ, Verrando P: Identification by cDNA microarray technology of genes modulated by artificial ultraviolet radiation in normal human melanocytes: Relation to melanocarcinogenesis. J Invest Dermatol 117:1471–1482, 2001

Venturelli D, Martinez R, Melotti P, et al: Overexpression of DR-nm23, a protein encoded by a member of the nm23 gene family, inhibits granulocyte differentiation and induces apoptosis in 32Dc13 myeloid cells. Proc Natl Acad Sci USA 92:7435–7439, 1995

Walker NJ: Real-time and quantitative PCR: Applications to mechanism-based toxicology. J Biochem Mol Toxicol 15:121–127, 2001

Wang N, Verna L, Hardy S, Zhu Y, Ma KS, Birrer MJ, Stemerman MB: c-Jun triggers apoptosis in human vascular endothelial cells. Circ Res 85:387–393, 1999

Wang SQ, Setlow R, Berwick M, Polsky D, Marghoob AA, Kopf AW, Bart RS: Ultraviolet A and melanoma: A review. J Am Acad Dermatol 44:837–846, 2001

Wendler WM, Kremmer E, Forster R, Winnacker EL: Identification of pirin, a novel highly conserved nuclear protein. J Biol Chem 272:8482–8489, 1997